



Research paper

Real-time Implementation of Sliding Mode Control for Cascaded Doubly Fed Induction Generator in both Islanded and Grid Connected Modes

H. Zahedi, G.R. Arab Markadeh*, S. Taghipoor

*Department of Engineering, Shahrekord University, Shahrekord, Iran.

Article Info

Article History:

Received 23 November 2019

Reviewed 02 January 2020

Revised 14 February 2020

Accepted 21 April 2020

Keywords:

Cascaded Doubly Fed Induction Generator (CDFIG)

Sliding Mode Control (SMC)

Grid-connected

Relative Gain Array (RGA)

Power control

*Corresponding Author's Email Address:

arab-gh@eng.sku.ac.ir

Abstract

Background and Objectives: Cascaded doubly fed induction generators (CDFIGs) can directly connected to isolated load or power grid without any brushes which are needed in conventional DFIGs. Output control targets before grid connection of CDFIGs are voltage and frequency control and after that are active and reactive power control. In control aspect, output control of CDFIG is a multi-input multi-output (MIMO) subject. In this paper, Relative Gain Array (RGA) methodology, as a MIMO interaction index, is used to show the degree of relevance between the control inputs and output targets, in both voltage control mode (before grid connection) and active-reactive power control mode (after grid connection). Based on RGA results, conventional PI controllers cannot be used to decouple control of generator outputs in grid connected mode. So, a powerful method based on sliding mode approach is proposed to generate the proper control voltages for output control of CDFIG in both islanded and grid connected mode. Simulation and experimental results using Matlab and TMS320F28335 based prototype of CDFIG are provided to demonstrate the effectiveness and robustness of the proposed method.

Methods: A mathematical method based on RGA matrix is used to evaluate the amount of interactions between output targets and input control variables in CDFIGs in islanded and grid connected mode.

Results: Conventional PI controller is a proper method to control the output voltage of Power Machine (PM) in CDFIG but is not a suitable technique for active and reactive power control in grid-tied mode.

Conclusion: Sliding mode control can be used to decouple control of CDFIGs in both before and after grid connection. As well as, robustness against the wind speed variation and parameters uncertainties is proved via both simulation and experimental tests.

©2020 JECEI. All rights reserved.

Introduction

Variable speed constant frequency (VSCF) operation is used in many industries that require Doubly Fed Induction Generators (DFIG). In these generators, even if there is a change of speed, they can be directly connected to the constant frequency grid using partially rated converters and rotor current regulation.

Therefore, they are useful for use in wind and hydropower systems [1].

However, the structure of these generators, which includes brushes and slip rings, reduces the life of the device due to the need for maintenance. Therefore, it is not quite suitable for use in applications such as aircraft, which require high reliability and long maintenance

period. In the CDFIG generator, by using two DFIGs and connecting the windings of the rotors to each other, a new brushless structure is obtained, which can be a suitable alternative to DFIG [2].

CDFIG works like a single DFIG so it can be connected directly to the network.

By connecting the two DFIG rotors mechanically and electrically, a CDFIG is obtained. DFIG machines are known as power machine and control machine [3].

The electric load or the grid is connected to the stator winding of the power machine (PM), and a power electronic converter supplies the stator winding of the control machine [4], Fig. 1.

Several studies on variable speed constant frequency generating system (VSCF) using CDFIG have been performed in applications such as windmills, hydropower and aircraft power supply [5].

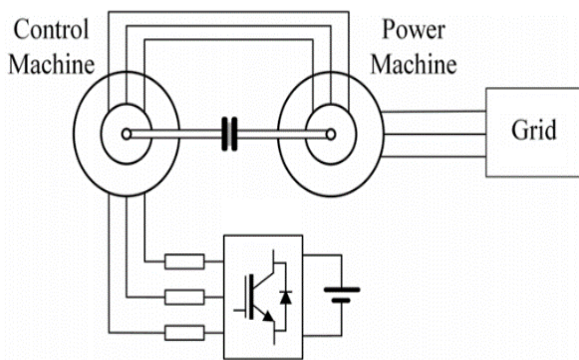


Fig. 1. CDFIG configuration.

The structure of CDFIG is complex in architecture and difficult to control, as well as, de-rating of the machine and higher price in comparison with DFIG. Therefore, despite its advantages, it is not widely used.

Due to the large size of the dynamic equation model, which is obtained by merging two DFIGs, the control of this machine has been influenced by its architecture [6].

A vector control method for DFIG is proposed in [7] and [8]. The method of improving the stability of multi-machine power network (MMPN) has been studied and the application of the conventional non-linear sliding mode control (SMC) is presented in [9].

The terminal SMC as a modified version of the conventional sliding mode control is presented in [10] for DFIG. In [11] by using the sliding mode method and estimating the position of the rotor, the DFIG is controlled. Efforts to control CDFIG have been limited, mainly based on field oriented control or vector control. In the vector control method, linear controllers such as PI regulate the components of the rotor currents, which include torque (or active power) and rotor flux (or reactive power) [12]-[13].

In [14], the active and reactive power of the power

machine is controlled based on vector control using PI controllers. But in this method, all of machine parameters are required in a recursive structure to generate the rotor reference currents and then the control machine reference currents. Also CDFIG is controlled based on DPC for wind energy applications in [15].

In MIMO system, as the interaction between each input with all outputs is high, the controller design will be complicated. As we know, in CDFIG the control inputs are the voltage of CM components and the outputs of plant are the active and reactive powers in grid connected mode or PM voltage components in islanded mode.

In this paper, using a powerful index named as Relative Gain Array (RGA), the decoupling index between the CM voltage components and the generator outputs is calculated. This index describes that the conventional controllers such as Proportional-Integrator (PI) especially in the grid-connected mode are not suitable for control of active and reactive power via PM voltages. Reference [16] used the RGA to calculate the degrees of relevance between the stator voltage and the stator flux of DFIG. The main contributions of this paper can be listed as:

- 1) The RGA indexes are calculated for output voltage control mode (in islanded mode) and active-reactive control mode (in grid connected mode). Therefore, the complexity of PI coefficients' tuning is clearly stated and proved with RGA index in grid connected mode. In this paper, based on the best knowledge of authors, for the first time, the clear relation between RGA index and complexity of control for CDFIG is reported.

- 2) In this paper, a sliding mode control is proposed to control the output active and reactive power of CDFIG. The required control voltage of the stator of control machine is calculated directly by the SMC method.

- 3) In the SMC method, the degree of controller system is decreased from order 6 to order 2, and using a proper Lyapunov function, the control voltage is obtained which is robust to system parameters. The robustness of SMC against the rotor resistance variation and rotor speed due to variable wind speed is proved.

- 4) The comparison of the proposed SMC and VC is done by experimental tests using a 370w CDFIG machine. Simulation and experimental results are presented to show the performance and robustness of the suggested control configuration during variations of operating point.

CDFIG Model

The two DFIMs have pole pair p_1 and p_2 respectively, with rotors connected in inverse coupling sequence. Then the voltages and currents of rotors can be written as:

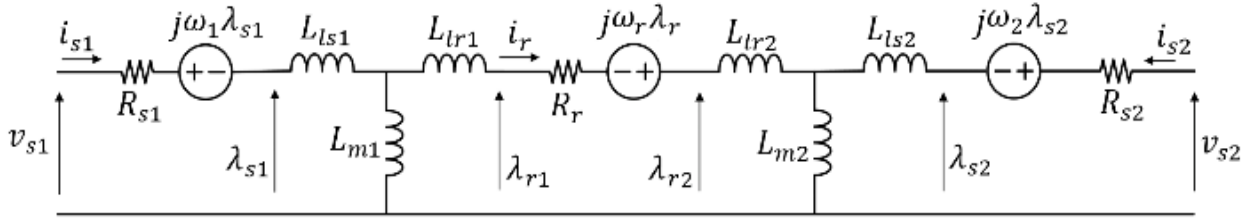


Fig. 2. Equivalent circuit of CDFIG.

$$\begin{aligned} v_{qr} &= v_{qr1} = v_{qr2} \\ v_{dr} &= v_{dr1} = -v_{dr2} \\ i_{qr} &= i_{qr1} = -i_{qr2} \\ i_{dr} &= i_{dr1} = i_{dr2} \end{aligned}$$

where v_{qr} , v_{dr} , i_{qr} and i_{dr} are the rotor voltage and rotor current components, respectively.

In order to specify the parameters of the two DFIM of the cascade, 1 and 2 subscriptions are used for all values in the system.

The subscripts s or r show the quantities of stator or rotor, and number 1 or 2 show the quantities of first or second machine, and q or d show the quantities of q-component or d-components.

Due to the d-components of stator voltage and q-component of rotor currents of control machine and power machine are in opposite sign.

The rotor is rotated at the mechanical angular frequency ω_m and the frequency of PM voltage is ω_1 . So, the flux that induced into the rotor bars has a frequency equal slip frequency of power machine that shown by (ω_r),

$$\omega_r = \omega_1 - p_1 \cdot \omega_m \quad (2)$$

Because the phase sequence is reversed at the rotor connection point, the flux wave frequency caused by the rotor control machine with the power machine slip frequency is in the opposite direction,

$$\omega_2 = -(\omega_1 - (p_1 + p_2) \cdot \omega_m) \quad (3)$$

In the other words, ω_m can be shown as

$$\omega_m = \frac{\omega_1 + \omega_2}{p_1 + p_2} \quad (4)$$

The behavior of CDFIG can be described by equations for each stator and combination of rotors. The complete CDFIG dynamic model in d-q reference frame can be given as:

$$\begin{aligned} v_{qs1} &= R_{s1} \cdot i_{qs1} + \frac{d}{dt} \lambda_{qs1} + \omega_1 \lambda_{ds1} \\ v_{ds1} &= R_{s1} \cdot i_{ds1} + \frac{d}{dt} \lambda_{ds1} - \omega_1 \lambda_{qs1} \\ v_{qs2} &= R_{s2} \cdot i_{qs2} + \frac{d}{dt} \lambda_{qs2} + \omega_2 \lambda_{ds2} \\ v_{ds2} &= R_{s2} \cdot i_{ds2} + \frac{d}{dt} \lambda_{ds2} - \omega_2 \lambda_{qs2} \end{aligned} \quad (5)$$

$$\begin{aligned} v_{qr} &= R_r \cdot i_{qr} + \frac{d}{dt} \lambda_{qr} + \omega_r \lambda_{dr} \\ v_{dr} &= R_r \cdot i_{dr} + \frac{d}{dt} \lambda_{dr} - \omega_r \lambda_{qr} \end{aligned}$$

where R , v , i and λ are the winding resistance, voltage, current and flow of control machine and power machine, respectively.

So, (5) can be written in matrix form as:

$$\dot{\Lambda} = V - R \cdot x - \Omega \cdot \Lambda \quad (6)$$

where

$$\Lambda = \begin{bmatrix} \lambda_{qs1} \\ \lambda_{ds1} \\ \lambda_{qs2} \\ \lambda_{ds2} \\ \lambda_{qr} \\ \lambda_{dr} \end{bmatrix}, \quad V = \begin{bmatrix} v_{qs1} \\ v_{ds1} \\ v_{qs2} \\ v_{ds2} \\ v_{qr} \\ v_{dr} \end{bmatrix}, \quad x = \begin{bmatrix} i_{qs1} \\ i_{ds1} \\ i_{qs2} \\ i_{ds2} \\ i_{qr} \\ i_{dr} \end{bmatrix} \quad (7)$$

$$R = \text{diag}[R_{s1} \quad R_{s1} \quad R_{s2} \quad R_{s2} \quad R_r \quad R_r]$$

$$\Omega = \text{diag}[\omega_1 \quad \omega_1 \quad \omega_2 \quad \omega_2 \quad \omega_r \quad \omega_r]$$

The stators and rotor flux vectors can be expressed as

$$\Lambda = L \cdot x \quad (8)$$

where

$$L = \begin{bmatrix} L_{s1} & 0 & 0 & 0 & L_m & 0 \\ 0 & L_{s1} & 0 & 0 & 0 & L_m \\ 0 & 0 & L_{s2} & 0 & -L_m & 0 \\ 0 & 0 & 0 & L_{s2} & 0 & L_m \\ -L_m & 0 & L_m & 0 & -L_r & 0 \\ 0 & L_m & 0 & L_m & 0 & L_r \end{bmatrix} \quad (9)$$

Then by substituting (9) into (8) and rearrange the equations, (6) can be rewritten based on the derivations of currents. The Equivalent circuit of CDFIG is shown in Fig. 2.

If the stator of power machine is connected to grid, then the active and reactive powers transferred to grid are calculated as

$$P = \left(\frac{3}{2}\right)(v_{ds1} \cdot i_{ds1} + v_{qs1} \cdot i_{qs1}) \quad (10)$$

$$Q = \left(\frac{3}{2}\right)(v_{qs1} \cdot i_{ds1} - v_{ds1} \cdot i_{qs1})$$

The q-axis of the synchronous reference frame is aligned to the phase "a" of grid voltage so the d-component of the grid voltage is always zero. By considering the grid voltage reference frame, $v_{ds1} = 0$. Then

$$P = \left(\frac{3}{2}\right)v_{qs1} \cdot i_{qs1} \quad (11)$$

$$Q = \left(\frac{3}{2}\right)v_{qs1} \cdot i_{ds1}$$

the entire MIMO system is controlled.

In the second method, the MIMO system is considered solid and does not decoupled into SISO systems. Therefore, the multivariate system controller, known as the concentrated control method, must be programmed simultaneously.

Bristol proposed the idea of Relative Gain Array (RGA) to measure the interaction between input and output pairing variables [17]. The system transfer matrix must be multiplied by the element in the inverse of its transposed matrix to obtain RGA. If an element of the RGA matrix is close to the unit, it shows that the input and output variables are a suitable pair that can form a control loop. In other words, a small positive RGA element indicates that the dependence between the input and output variables is low [18].

$$\begin{bmatrix} y_1 \\ y_2 \end{bmatrix} = G(s) \cdot \begin{bmatrix} u_1 \\ u_2 \end{bmatrix} \quad (12)$$

$$G(s) = \begin{bmatrix} g_{11} & g_{12} \\ g_{21} & g_{22} \end{bmatrix}$$

$$RGA = G(s) \cdot \times (G(s)^T)^{-1}$$

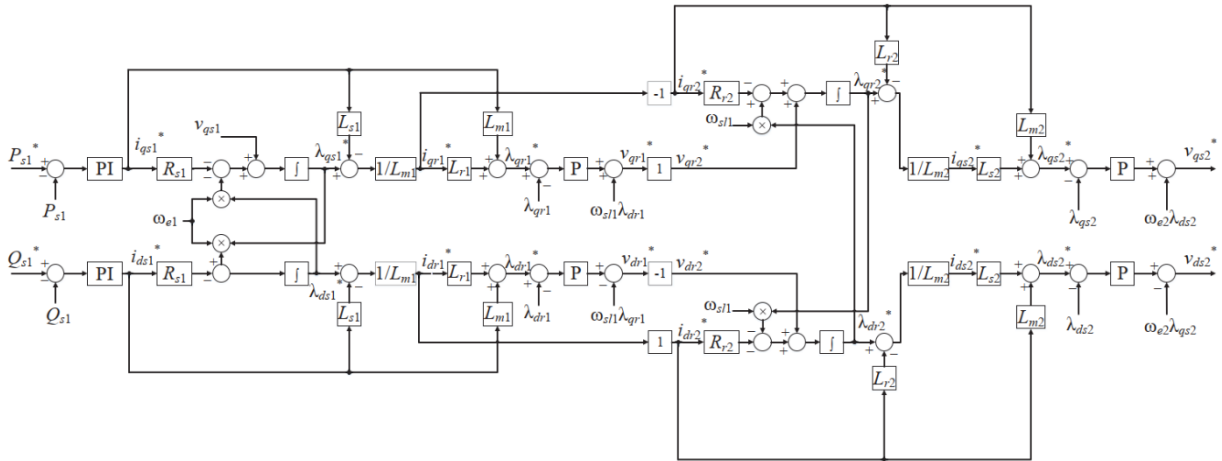


Fig. 3: Vector Control Method by Lipo [14].

Interaction between input and output

In multivariate systems, the interaction between input and output pairing variables is the main problem. This limitation can be overcome by planning suitable controllers for these systems in two main methods.

The first method is to try to convert the MIMO system to several SISO systems. Therefore, the system must be decoupled to eliminate interactions between input and output pairing variables.

By properly measuring the interaction between the input and output variables, the appropriate input and output pairing variables are selected. In this way, the system is decoupled into other SISO systems. A controller is then programmed for each loop, and finally

In this paper the designing stages of multivariable control systems for non-minimum phase are studied.

The theories represented for decoupling multivariable systems can be applied only for minimum phase systems, and are not valid for non-minimum phase systems.

A. Before Grid Connection (Islanded mode)

Before connection of CDFIG output to grid or in islanded mode, the voltage magnitude, frequency and the voltage phase should be the same as grid ones.

When CDFIG is not connected to grid, the aim of controller is to control the terminal voltage of power machine. So, the inputs are voltage of control machine, v_{qs2} and v_{ds2} , and the outputs are voltage of power

machine component, v_{qs1} and v_{ds1} .

$$\begin{bmatrix} v_{qs1} \\ v_{ds1} \end{bmatrix} = G_{IS}(s) \cdot \begin{bmatrix} v_{qs2} \\ v_{ds2} \end{bmatrix} \quad (13)$$

Then, using the system parameters listed in Table 1. RGA is calculated by (12) as follow:

$$RGA_{IS} = \begin{bmatrix} 0.9324 & 0.0676 \\ 0.0676 & 0.9324 \end{bmatrix}$$

The diagonal elements have the values close to unit and off-diagonal elements have the values close to zero in RGA_{IS} . Therefore, for the controller, the appropriate input and output pairs in (13) should be considered direct to direct voltage and the quadrature to quadrature voltage of the power and the control machine, respectively.

power, P and Q.

$$\begin{bmatrix} P_s \\ Q_s \end{bmatrix} = G_{GC}(s) \cdot \begin{bmatrix} v_{qs2} \\ v_{ds2} \end{bmatrix} \quad (14)$$

Then the RGA in this case is calculated by (12) as follow:

$$RGA_{GC} = \begin{bmatrix} 0.7487 & 0.2513 \\ 0.2513 & 0.7487 \end{bmatrix}$$

Therefore, since the RGA_{GC} is off-diagonal and not a near unitary matrix, the dependency between inputs and outputs is high.

Then the conventional cascaded PI control method isn't suitable for this machine.

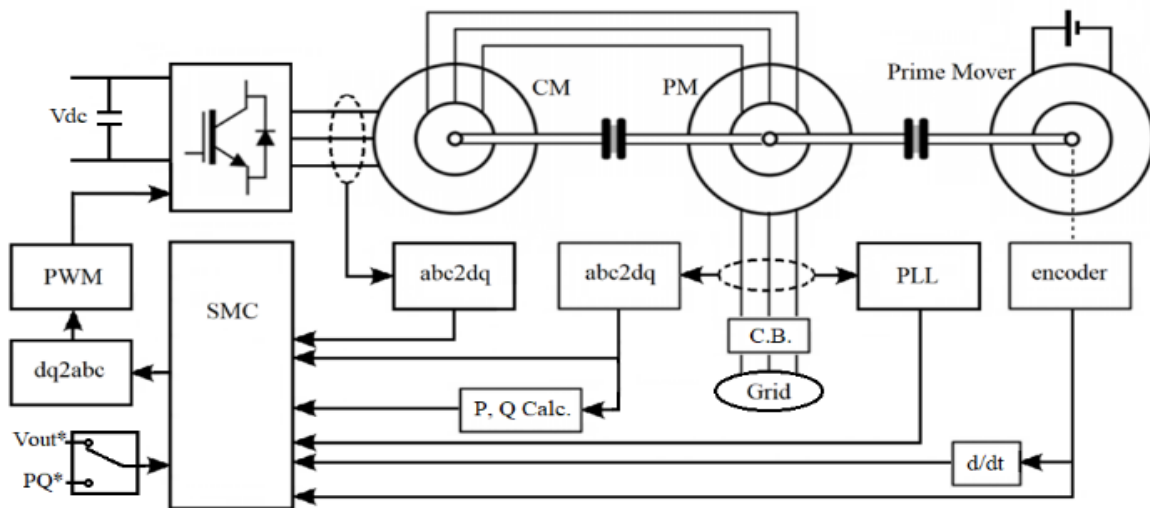


Fig. 4: Block diagram of SMC for CDFIG in islanded and grid connected mode.

So, in this case the cross correlation between inputs and outputs is low. In the other word, the v_{qs2} has low interaction on v_{ds1} and also like to v_{ds2} on v_{qs1} . Then the plant can be controlled by two decoupled conventional PI controllers.

B. After Grid Connection

To connect the generator to grid, it is necessary to synchronize the power machine voltage with the grid, and then transferring the active and reactive with grid.

In [19], only deals with stand-alone mode for DFIG. However, the complexity of the equations and the dependence of the inputs and outputs are mostly determined in the grid-connected mode.

Calculation of RGA in grid connected mode confirms this.

For CDFIG system, when it is connected to grid, the input signals are terminal voltage of control machine, v_{qs2} and v_{ds2} , and the outputs are active and reactive

Sliding Mode Control

In [14] a vector control for CDFIG is presented. As can be seen in Fig. 3, the controller is deeply dependent to parameters of machine. The controller is required the instantaneous rotor flux to be used as the feedback signal, which forces additional rotor-flux observer. Also, all of machine parameters are required in a recursive structure to generate the rotor reference currents and then the control machine reference currents using four P and two PI controllers can be calculated. So the tuning of PI coefficients is the main drawback of that method. The SMC is designed based on selecting a hyper plane in the state space or error space (called the sliding surface). If the state trajectory is confined to it, it will slide to the desired equilibrium point. By applying a control law based on sliding mode technique the system state is transferred to the sliding surface (in reaching mode) from an arbitrary initial condition and then, stays on (or close to) the sliding surface for all times and moves towards the equilibrium point (in sliding mode).

A. Before Grid Connection

The main target for SMC approach in islanded mode is to regulate the power machine voltage components in desired values, $v_{ds1} = v_{dref}$ and $v_{qs1} = v_{qref}$.

The sliding surfaces are selected in the integral forms as

$$\begin{aligned} S_d &= e_d(t) + K_d \cdot \int e_d(t) dt \\ S_q &= e_q(t) + K_q \cdot \int e_q(t) dt \end{aligned} \quad (15)$$

where K_d and K_q are constant positive gains, and $e_d(t)$ and $e_q(t)$ are the differences between references and actual values of power machine voltage components, respectively.

$$e_d = v_{dref} - v_{ds1}$$

$$e_q = v_{qref} - v_{qs1}$$

Based on control design methods for sliding mode approach [19], the proper voltage references for VSI which feeds the control machine windings can be obtained as follows:

$$\begin{bmatrix} v_{qs2} \\ v_{ds2} \end{bmatrix} = -M^{-1} \cdot \left(N + \begin{bmatrix} K_d \cdot \text{sgn}(S_d) \\ K_q \cdot \text{sgn}(S_q) \end{bmatrix} \right) \quad (16)$$

where M and N can be calculated like as stated for grid connected mode in appendix.

The step by step design procedure will be explained for grid-connected mode and is ignored because of similarity.

B. After Grid Connection

After grid connection, the control targets are the active and reactive power transferred to grid via power machine. Also the control inputs are the components of control machine voltages, v_{qs2} and v_{ds2} .

The Time derivative of P and Q can be obtained as

$$\begin{aligned} \dot{P} &= \left(\frac{3}{2}\right) (v_{qs1} \cdot i_{qs1} + v_{qs1} \cdot i_{qs1}) \\ \dot{Q} &= \left(\frac{3}{2}\right) (v_{qs1} \cdot i_{ds1} + v_{qs1} \cdot i_{ds1}) \end{aligned} \quad (17)$$

By considering $v_{qs1} = V_m$ and $v_{qs1} = 0$, then

$$\begin{aligned} \dot{P} &= \left(\frac{3}{2}\right) V_m \cdot i_{qs1} \\ \dot{Q} &= \left(\frac{3}{2}\right) V_m \cdot i_{ds1} \end{aligned} \quad (18)$$

As the main task of the SMC approach, the active and reactive power must follow the reference values. Therefore, the sliding surface vector is given below:

$$S = \begin{bmatrix} S_p \\ S_q \end{bmatrix} \quad (19)$$

The sliding surfaces are assumed in the integral forms,

$$\begin{aligned} S_p &= e_p(t) + K_p \cdot \int e_p(t) dt \\ S_q &= e_q(t) + K_q \cdot \int e_q(t) dt \end{aligned} \quad (20)$$

where K_p and K_q are constant positive gains, and $e_p(t)$ and $e_q(t)$ are the differences between references and actual values of active and reactive power respectively.

$$e_p = P_{ref} - P \quad (21)$$

$$e_q = Q_{ref} - Q$$

when the system states achieve the desired surface, then we have:

$$\begin{aligned} S_p &= \dot{S}_p = 0 \\ S_q &= \dot{S}_q = 0 \end{aligned} \quad (22)$$

If the control laws are selected properly, we have

$$\begin{aligned} \dot{e}_p &= -K_p \cdot e_p \\ \dot{e}_q &= -K_q \cdot e_q \end{aligned} \quad (23)$$

It means that the errors will converge exponentially to zero.

According to (23)

$$\begin{aligned} \dot{S}_p &= \dot{e}_p + K_p \cdot e_p = -\dot{P} + K_p \cdot (P_{ref} - P) \\ \dot{S}_q &= \dot{e}_q + K_q \cdot e_q = -\dot{Q} + K_q \cdot (Q_{ref} - Q) \end{aligned} \quad (24)$$

Substituting (18) into (24) yields

$$\dot{S} = E + F \cdot U \quad (25)$$

With

$$\begin{aligned} E &= [E_{2 \times 1}] \\ F &= [F_{2 \times 2}] \\ U &= \begin{bmatrix} v_{qs2} \\ v_{ds2} \end{bmatrix} \end{aligned} \quad (26)$$

where E and F are stated in appendix.

By applying Lyapunov theory in SMC method, the conditions of control law are derived and the state trajectory towards the desired behavior. Consider the quadratic function of Lyapunov as follows:

$$W = \frac{1}{2} S^T S \quad (27)$$

The time derivative of W of (22) is expressed as

$$\dot{W} = \frac{1}{2} (\dot{S}^T \dot{S} + S^T \dot{S}) \quad (28)$$

The control law should be selected so that the time derivative of W is negative definite with $S \neq 0$. Thus, the control law is selected as follow:

$$\begin{bmatrix} v_{qs2} \\ v_{ds2} \end{bmatrix} = -F^{-1} \cdot \left(E + \begin{bmatrix} K_P \cdot \text{sgn}(S_P) \\ K_Q \cdot \text{sgn}(S_Q) \end{bmatrix} \right) \quad (29)$$

Where K_P and K_Q are positive control gains, $\text{sgn}(S_P)$ and $\text{sgn}(S_Q)$ are switching functions for active and reactive powers respectively. The block diagram of SMC for CDFIG is depicted in Fig. 4.

In order to decrease the chattering phenomena, the discontinues sign function can be replaced with saturation function. The reference voltage that is obtained from (29) can be used to drive the stator of control machine.

Simulation Results

Simulation of the proposed control strategy based on Fig. 4 is carried out by MATLAB/Simulink. Discrete model is used with a simulation time step of 20 μ s. The machine parameters are listed in Table 1.

Table 1: CDFIG parameters

Parameter	Value
V	220 V
Rs1	1.6 Ω
Rs2	1.6 Ω
Rr	3.2 Ω
p ₁	1
p ₂	1
L _{ls1}	0.004 H
L _{ls2}	0.004 H
L _{lr}	0.008 H
L _m	0.125 H

A. Before Grid Connection

The controller is used to control the stator voltage of power machine using the voltage source inverter which supplies the control machine windings. In this step, the first condition for grid connection, which is PM voltage equal to grid voltage, can be obtained.

The terminal voltage of the PM must be in the range of 220 volts and a frequency of 50 Hz and be in-phase with the grid voltage.

Terminal voltage of power machine in islanded mode

with PI and SMC are shown in Fig. 5. Both of SMC and PI controller can control the voltage of CDFIG. But the dynamic response of PI controller is slower than SMC. As can be seen, the rise time of dynamic response with PI and SMC are 0.2 and 0.03 sec respectively.

B. After grid Connection

After connection of CDFIG to grid, the controller must track the active and reactive power references. Considering the steady-state operation of the CDFIG with defined parameters as Table 1, the output active power reference is stepped up from 0.5 pu to 1.0 pu at t=1 s, and stepped down from 1.0 pu to 0.5 pu at t=1.5 s. As well as, the output reactive power reference is set to zero. Simulation results for active and reactive power control are shown in Figs. 5 and 6. For this condition, the obtained results are demonstrated by vector control and sliding mode control in Fig. 6 and Fig. 7, respectively. It can be seen, the output active and reactive powers follow the reference values in both methods, but SMC is so accurate and rapid. It is shown, the rise time of dynamic response with PI and SMC are 0.05 sec and 0.0003 sec respectively. As well as, the steady state error in two methods are zero. The overshoot in active power control with PI is about 10% and in SMC is also 10%. Furthermore, as can be seen in Fig. 6b and Fig. 7b, the fluctuation in reactive power when the active power reference is changed with step command is shown about 50% with PI controller while in SMC method no variation in reactive power is shown in the same condition of active power reference changes. It means the active and reactive power controllers are exactly decoupled in SMC method, while in vector control method the controllers are coupled, especially in transient regions.

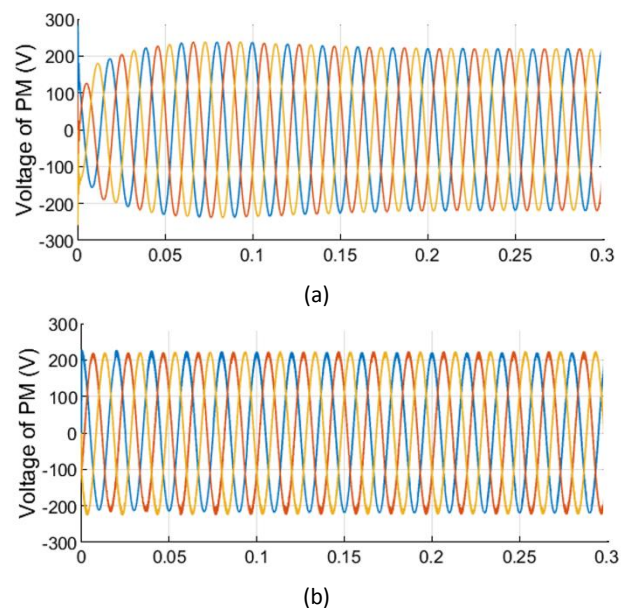


Fig. 5. Simulation results: Three phase Voltage of Power Machine Terminal. (a) Vector Control Method, (b) SMC Method.

C. Robustness against parameters uncertainties

In order to show the effectiveness of SMC against parameter uncertainties, a step change in rotor resistance is assumed and then the output behavior is depicted. Considering the active and reactive power is constant. At $t=1.0$ sec rotor resistance value is increased around 20 percent, from 3.2Ω to 3.84Ω . Simulation results are illustrated in Fig. 8. The output active and reactive power as well as their reference values, are depicted.

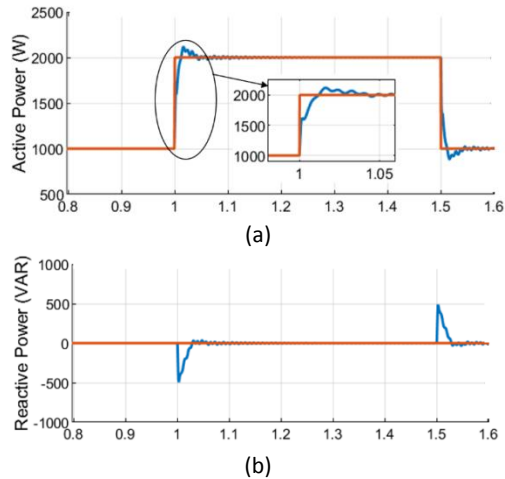


Fig. 6. Simulation results: Active and Reactive Power with step change in reference values by Vector Control Method.

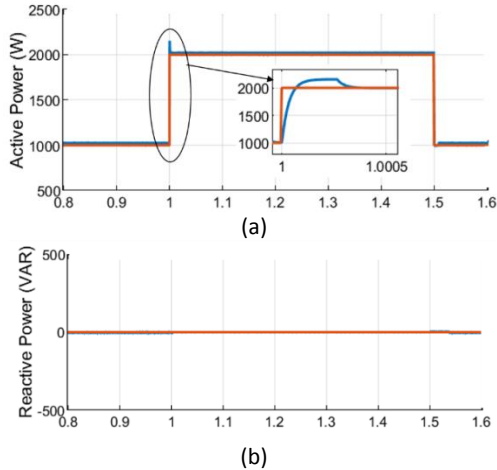


Fig. 7. Simulation results: Active and Reactive Power with step change in reference values by SMC Method; a) Active power, b) Reactive power.

As can be seen, there very small fluctuations in the active and reactive power are shown, that verifies the performance of SMC.

Experimental Result

The performance of the proposed SMC is verified by a DSP-based prototype of CDFIG and its controller as depicted in Fig. 9. The practical setup consists of two DFIGs 370 W with cross interconnected rotor windings for implementation of CDFIG, one DC motor as a prime

mover, voltage source inverter with its driver board to supplying the control machine, current and voltage sensor boards and a TMS320F28335 discrete signal processor board.

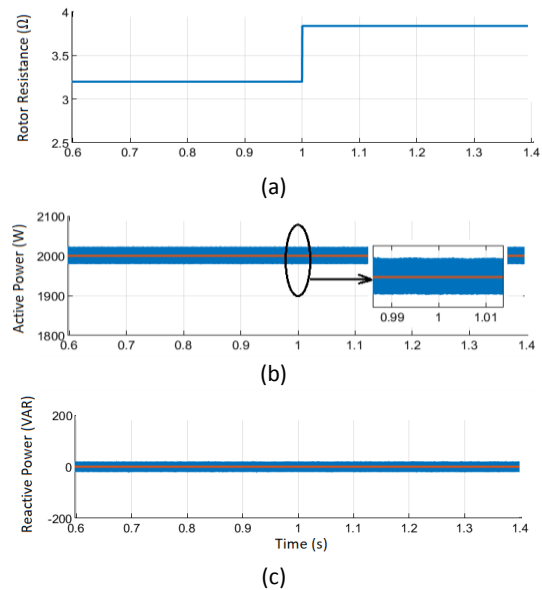


Fig. 8. Simulation results: P & Q control with increase in rotor resistance (SMC); a) Rotor resistance step change, b) Active power, c) Reactive power.

Two Hall-effect current sensors (LEM LA-55P) are measured the power machine currents, and a voltage sensor (LEM LV-25P) is calculated the line-to-line voltage. The analog second-order low pass filters are used to filtered the measured stator currents and voltage signals, with cut-off frequency of about 2.6 kHz, and converted to digital by 12-bit on-chip A/D converters.

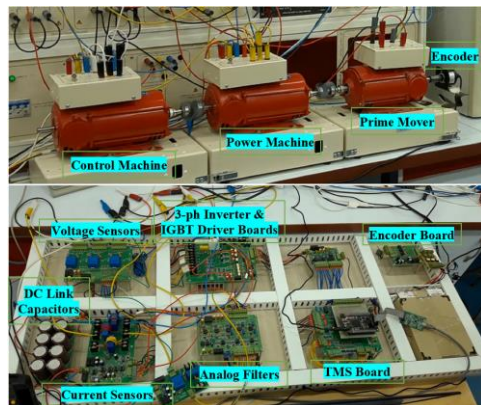


Fig. 9. Experimental setup of the grid connected CDFIG.

An incremental encoder with 1024 pulses per round connected to the DC motor shaft measures the rotor speed. The three phase inverter used in this setup includes six low loss IGBT switches kth123 (with 80 A, 1200 V ratings). Also, intelligent IGBT drivers, HCPL-316J, is used in this inverter which guarantee electrical separation between the power and control systems. The switching frequency of the inverter is selected as 10 kHz.

A. Before grid connection

The TMS board is used to control the stator voltage of power machine by a VSI which is connected to control machine. The terminal voltage of PM should be synchronized with the grid voltage. In order to ensuring the grid synchronization of power machine, Phase-Locked Loop (PLL) is used. Grid voltage is transformed to dq-synchronous rotating reference frame using Park transformation with estimated phase angle from the PLL output. Fig. 10 shows the grid and the CDFIG voltages before connection together.

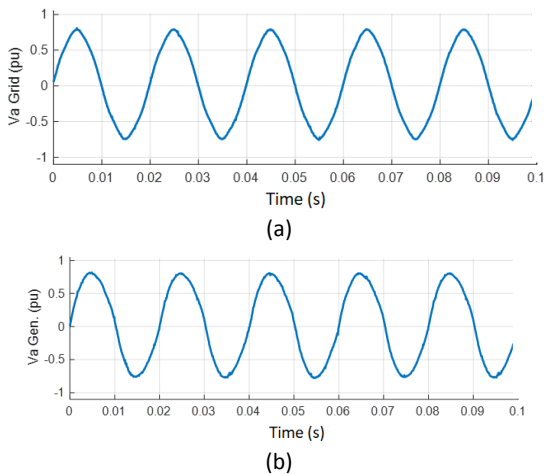


Fig. 10. Experimental results of Grid and Power machine terminal before connected together; (a) Grid Voltage, (b) Power Machine Voltage.

In order to show the effectiveness of SMC for output voltage control before connection to grid, the speed of prime mover is changed from 0.6 pu to 1 pu. Fig. 11 shows that, during the speed variation, the PM output voltage and frequency are controlled, but the Control machine current frequency decreases proportional to the CDFIG slip changes. Therefore, the robustness of proposed SMC against the rotor speed variation is verified.

B. Step change in output voltage in islanded mode

Controllability of terminal voltage of PM is verified by change in output reference voltage. Fig. 12 shows the output voltage of PM with a step change in references from -0.4 pu to 0.4 pu at t=10 s. In grid-tied mode, the active power reference is stepped up from 0.4 pu to 0.9 pu at t=2 s and stepped down from 0.9 pu to 0.4 pu at t=13 s. The reactive power reference is set to zero. Experimental results for vector control and sliding mode control are shown in Fig. 14.

C. Active and Reactive power control in grid connected mode

As can be seen, the rise time of dynamic response with PI and SMC are 2 and 0.2 sec respectively.

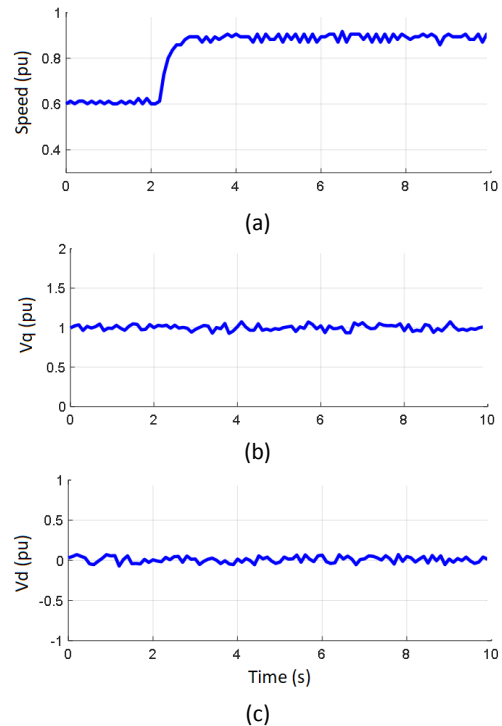


Fig. 11. Experimental result for speed change; (a) Speed of rotor, (b) Voltage of q-axis, (c) Voltage of d-axis.

This results show that the proposed SMC has very fast dynamic response in active power control. Also the interaction between active and reactive power is very low.

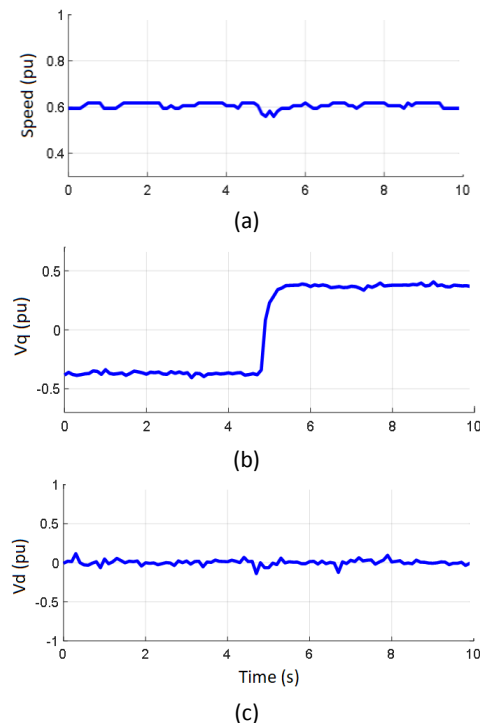


Fig. 12. Experimental result for voltage Ref. change; (a) Speed, (b) Voltage of q-axis, (c) Voltage of d-axis.

Fig. 13 shows the instantaneous output voltage of PM versus time.

The overall results are shown in the Table 2.

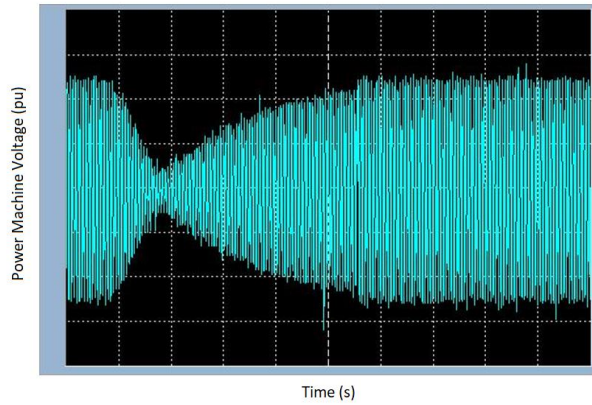


Fig. 13. Change in voltage reference from -0.4 pu to +0.4 pu.

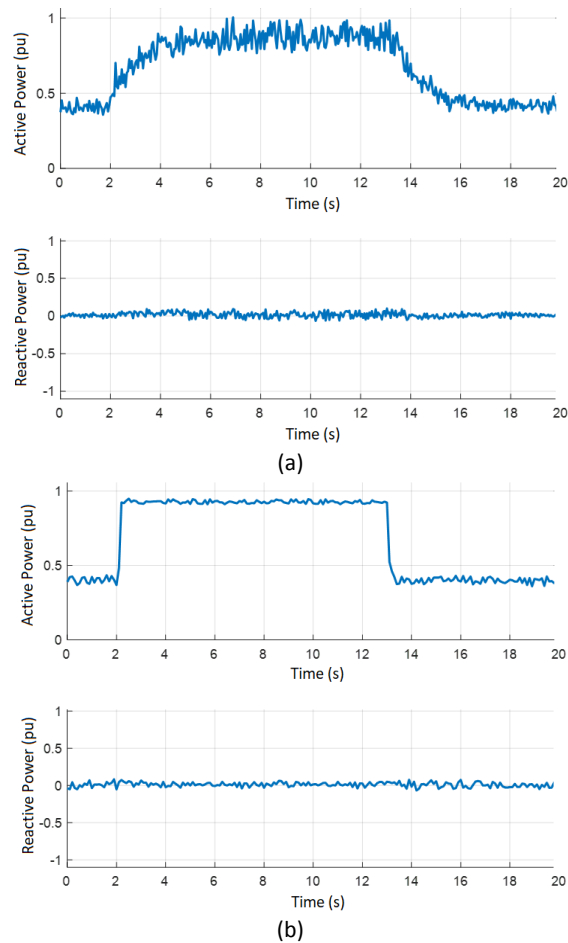


Fig. 14. Experimental results for changes active power reference at $t=2s$ and $t=13s$; (a) vector control, (b) Sliding Mode Control.

Table 2: Simulation results

Parameter	PI	SMC
Voltage rise time (sim.)	0.2	0.03
Power rise time (sim.)	0.05	0.0003
Power rise time (exp.)	2	0.2

Conclusion

In this paper for the first effort, the RGA index is calculated to determine the interaction between the stator voltages of power machine and control machine in CDFIGs. The RGA index in islanded mode is near to diagonal matrix form and results a successful decoupled control for voltage control mode. While its results for grid-connected mode shows a huge interaction between all inputs and outputs, so the plant cannot be properly controlled by conventional PI controller. Therefore, the proposed sliding mode controller can be used to track the CDFIG targets in both islanded and grid-connected mode. As well as, the proposed method is robust to motor parameters uncertainties and has higher dynamic response in comparison with conventional vector control using PI regulators. Also, the effectiveness of the SMC method is verified by some simulation and experimental results, with variable wind speed and step changes in output targets.

Author Contributions

H. Zahedi, G.R. Arab Markadeh implemented the experimental setup and designed the simulations and experiments. S. Taghipoor, designed the CDFIG simulation model.

Acknowledgment

The authors wish to acknowledge the Shahrekord Univ. Supports.

Abbreviations

$v_{qs1} \cdot v_{ds1}$	Voltages of d- and q- axis of power machine
$v_{qs2} \cdot v_{qs2}$	Voltages of d- and q- axis of control machine
$v_{qr} \cdot v_{dr}$	Voltages of d- and q- axis of rotor
$i_{qs1} \cdot i_{ds1}$	Currents of d- and q- axis of power machine
$i_{qs2} \cdot i_{qs2}$	Currents of d- and q- axis of control machine
$i_{qr} \cdot i_{dr}$	Currents of d- and q- axis of rotor
$\lambda_{qs1} \cdot \lambda_{ds1}$	Fluxes of d- and q- axis of power machine
$\lambda_{qs2} \cdot \lambda_{ds2}$	Fluxes of d- and q- axis of control machine
$\lambda_{qr} \cdot \lambda_{dr}$	Fluxes of d- and q- axis of rotor
$\omega_1 \cdot \omega_2$	Frequency of power and control machine
ω_m	Mechanical angular frequency
ω_r	Frequency of rotor flux

Appendix

A. Current Model

Current model for CDFIG can be described as

$$\begin{aligned} \dot{x} &= A \cdot x + B \cdot u \\ y &= C \cdot x \end{aligned} \quad (A1)$$

where A , B and C are described in (A2), u is $[v_{qs2} \ v_{ds2}]^T$ and $y = [P_s \ Q_s]^T$ for grid connected and $y = [v_{qs1} \ v_{ds1}]^T$ for isolated load.

$$A = \frac{1}{L_a} [a_{ij}] \quad : \quad i, j = 1 \dots 6$$

$$B = \frac{1}{L_a} \begin{bmatrix} -L_m^2/L_s & 0 \\ 0 & L_m^2/L_s \\ L_b/L_s & 0 \\ 0 & L_b/L_s \\ L_m & 0 \\ 0 & -L_m \end{bmatrix} \quad (A2)$$

$$C = (2/3)v_{qs1} \begin{bmatrix} 1 & 0 & 0 & 0 & 0 & 0 \\ 0 & 1 & 0 & 0 & 0 & 0 \end{bmatrix}$$

By define $L_a = 2(L_r L_s - L_m^2)$, $L_b = 2L_r L_s - L_m^2$ and

$$\begin{aligned} a_{11} &= a_{22} = a_{33} = a_{44} = -R_s * L_b / L_s \\ a_{12} &= -a_{21} = -L_m^2 * \omega_m - L_a * \omega_s \\ a_{13} &= -a_{24} = a_{31} = -a_{42} = L_m^2 * R_s / L_s \\ a_{14} &= a_{23} = a_{32} = a_{41} = L_m^2 * \omega_m \\ a_{34} &= -a_{43} = -L_m^2 * \omega_m - L_a * (2\omega_m - \omega_s) \\ a_{15} &= a_{26} = -a_{35} = a_{46} = L_m * R_r \\ a_{16} &= -a_{25} = a_{36} = a_{45} = -L_m * \omega_m * L_a / L_s \\ a_{51} &= a_{62} = -a_{53} = a_{64} = L_m * R_s \\ a_{52} &= -a_{61} = -a_{63} = -a_{54} = L_m * L_s * \omega_m \\ a_{55} &= a_{66} = -L_s * R_r \\ a_{56} &= -a_{65} = -L_a * (\omega_m - \omega_s) \end{aligned} \quad (A3)$$

The system output is the active and reactive power generated by CDFIG, that related to direct and quadrature current components of power machine. Therefore, the matrix C is shown in (A2).

B. Matrix E and F

$$\text{By define } L_c = 4L_r L_s - L_m^2$$

$$E = \frac{1}{4L_s L_b} \begin{bmatrix} E_1 \\ E_2 \end{bmatrix}$$

$$F = \begin{bmatrix} L_m^2 & 0 \\ 0 & L_m^2 \end{bmatrix} \quad (A3)$$

where

$$\begin{aligned} A_1 &= L_c L_s \omega_s i_{qs1} + L_c R_s i_{ds1} + L_m^2 L_s \omega_m i_{qs2} \\ &\quad - L_m^2 R_s i_{ds2} + 2L_m L_b \omega_m i_{qr} \\ &\quad + (L_m^2 L_s (\omega_m - \omega_s) + L_m L_s R_r) i_{dr} \\ A_2 &= L_c L_s \omega_s i_{ds1} + L_c R_s i_{qs1} + L_m^2 L_s \omega_m i_{qs2} \\ &\quad - L_m^2 R_s i_{ds2} + 2L_m L_b \omega_m i_{dr} \\ &\quad + (L_m^2 L_s (\omega_m - \omega_s) + L_m L_s R_r) i_{qr} \end{aligned} \quad (A4)$$

References

[1] F. Blaabjerg, M. Liserre, K. Ma, "Power electronics converters for wind turbine systems," *IEEE Trans. Ind. Appl.*, 48(2): 708–719, 2012.

- [2] B. Hopfensperger, D. J. Atkinson, R. A. Lakin, "Stator flux oriented control of a cascaded doubly-fed induction machine," *Proc. Inst. Elect. Eng.—Elect. Power Appl.*, 146(6): 597–605, 1999.
- [3] T. D. Strous, H. Polinder, J. A. Ferreira, "Brushless doubly-fed induction machines for wind turbines: developments and research challenges," in *IET Electric Power Applications*, 11(6): 991–1000, 2017.
- [4] E. Abdi, R. McMahan, P. Malliband, S. Shao, M. E. Mathekg, P. Tavner, S. Abdi, A. Oraee, T. Long, M. Tatlow, "Performance analysis and testing of a 250 kw medium-speed brushless doubly-fed induction generator," *IET Renew. Power Gener.*, 7(6): 631–638, 2013.
- [5] M. Achkar, R. Mbayed, G. Salloum, S. Le Ballois, E. Monmasson, "Generic study of the power capability of a cascaded doubly fed induction machine," *International Journal of Electrical Power & Energy Systems*, 86: 61–70, 2017.
- [6] S. Ademi, M. G. Jovanović, M. Hasan, "Control of Brushless Doubly-Fed Reluctance Generators for Wind Energy Conversion Systems," in *IEEE Transactions on Energy Conversion*, 30(2): 596–604, 2015.
- [7] Y. Tang, H. He, Z. Ni, J. Wen, X. Sui, "Reactive power control of grid-connected wind farm based on adaptive dynamic programming," *Neurocomputing*, 125: 125–133, 2014.
- [8] J. Chen, W. Zhang, B. Chen, Y. Ma, "Improved vector control of brushless doubly fed induction generator under unbalanced grid conditions for offshore wind power generation," *Energy Conversion, IEEE Transactions on*, 31(1): 293–302, 2015.
- [9] J.d.D.N. Ndongmo, G. Kenné, R.K. Fochie, A. Cheukem, H.B. Futsin, F.L. Lagarrigue, "A simplified nonlinear controller for transient stability enhancement of multimachine power systems using SSSC device," *Int. J. Electr. Power Energy Syst.*, 54: 650–657, 2014.
- [10] G. Wang, R. Wai, Y. Liao, "Design of backstepping power control for grid-side converter of voltage source converter-based high-voltage dc wind power generation system," in *IET Renewable Power Generation*, 7(2): 118–133, 2013.
- [11] H. E. Medouce, H. Benalla, A. Mehdi, A. Reama, "Sensorless direct power regulation by sliding mode approach of DFIG generator based wind energy system," in *Proc. 2015 IEEE 15th International Conference on Environment and Electrical Engineering (EEEIC), Rome: 1880–1885, 2015.*
- [12] Z. TIR, H. Rajeai, R. Abdessemed, "Analysis and vector control of a cascaded doubly fed induction generator in wind energy applications". *Revue des Energies Renouvelables*: 347–358, 2010.
- [13] M. E. Achkar, R. Mbayed, G. Salloum, N. Patin, S. Le Ballois, E. Monmasson, "Modeling and control of a stand alone cascaded doubly fed induction generator supplying an isolated load," 2015 17th European Conference on Power Electronics and Applications (EPE'15 ECCE-Europe), Geneva: 1–10, 2015.
- [14] Z. S. Du, T. A. Lipo, "Dynamics and vector control of wound-rotor brushless doubly fed induction machines," in *Proc. 2014 IEEE Energy Conversion Congress and Exposition (ECCE), Pittsburgh, PA: 1332–1339, 2014.*
- [15] J. Hu, J. Zhu, D. G. Dorrell, "A New Control Method of Cascaded Brushless Doubly Fed Induction Generators Using Direct Power Control," in *IEEE Transactions on Energy Conversion*, 29(3): 771–779, 2014.
- [16] K. C. Wong, S. L. Ho, K. W. E. Cheng, "Direct voltage control for grid synchronization of doubly-fed induction generators," *Electr. Power Compon. Syst.*, 36(9): 960–976, 2008.

- [17] M. Sadrnia, "A novel method for decoupling of non-minimum phase MIMO systems": 475-480, 2006.
- [18] S. Z. Chen, N. C. Cheung, Y. Zhang, M. Zhang, X. M. Tang, "Improved Grid Synchronization Control of Doubly Fed Induction Generator Under Unbalanced Grid Voltage," in IEEE Transactions on Energy Conversion, 26(3): 799-810, 2011.
- [19] S. Z. Chen, N. C. Cheung, K. C. Wong, J. Wu, "Grid Synchronization of Doubly-fed Induction Generator Using Integral Variable Structure Control," in IEEE Transactions on Energy Conversion, 24(4): 875-883, 2009.

Biographies



Hossein Zahedi Abdolhadi received the B.S. degree in Electrical Engineering from the University of Kashan, Kashan, Iran, in 2007 and the M.S. degree in Electrical Engineering from Tarbiat Modares University, Tehran, Iran, in 2010. He is currently working toward the PhD degree in the Faculty of Engineering, Shahrekord University, Shahrekord, Iran. His research interests include power converters,

motor drivers and nonlinear control as well as control of power electronics and electric drives using microcontrollers and DSPs.



Gholamreza Arab Markadeh received the B.Sc., M.Sc., and Ph.D. degrees in Electrical Engineering from Isfahan University of Technology, Iran, in 1996, 1998, and 2005, respectively. He is currently an Associate Professor in the Faculty of Engineering, Shahrekord University. His fields of research include nonlinear control, power electronics, and variable-speed drives. He is the Editor-in-chief of Journal of Dam and Hydroelectric Powerplant. Dr. Arab Markadeh was the recipient of the IEEE Industrial Electronics Society IECON'04 best paper presentation award in 2004.



Samad Taghipour Boroujeni received the B.Sc, M.Sc., and Ph.D. degrees in electrical engineering from the Department of Electrical Engineering, Amirkabir University (Tehran Polytechnic), Tehran, Iran, in 2003, 2005, and 2009, respectively. In 2009, he joined the Department of Engineering, Shahrekord University, Shahrekord, Iran, as an Assistant Professor. Since 2016, he has been working as an

Associate Professor. His research interests include modeling, design, analysis, optimization, and control of electrical machines, especially variable-speed generators.

Copyrights

©2020 The author(s). This is an open access article distributed under the terms of the Creative Commons Attribution (CC BY 4.0), which permits unrestricted use, distribution, and reproduction in any medium, as long as the original authors and source are cited. No permission is required from the authors or the publishers.



How to cite this paper:

H. Zahedi, G.R. Arab Markadeh, S. Taghipoor, "Real-time Implementation of Sliding Mode Control for Cascaded Doubly Fed Induction Generator in both Islanded and Grid Connected Modes," Journal of Electrical and Computer Engineering Innovations, 8(2): 285-296, 2020.

DOI: [10.22061/JECEI.2020.7361.384](https://doi.org/10.22061/JECEI.2020.7361.384)

URL: http://jecei.sru.ac.ir/article_1476.html

